Induction of a G_1-S checkpoint in fission yeast

Cathrine A. Bøe[a,b], Marit Krohn[a,b], Gro Elise Rødland[a,b], Christoph Capiaghi[c,1], Olivier Maillard[c], Fritz Thoma[c], Erik Boye[a,2], and Beáta Grallert[a,b]

[a]Department of Cell Biology, Institute for Cancer Research, Oslo University Hospital, Montebello, 0310 Oslo, Norway; [b]Institute for Molecular Biosciences, University of Oslo, 0316 Oslo, Norway; and [c]Department of Biology, Institute of Molecular Health Science, Eidgenössische Technische Hochschule (ETH) Zürich, CH-8093 Zürich, Switzerland

Edited* by Nancy E. Kleckner, Harvard University, Cambridge, MA, and approved May 3, 2012 (received for review March 27, 2012)

Entry into S phase is carefully regulated and, in most organisms, under the control of a G_1-S checkpoint. We have previously described a G_1-S checkpoint in fission yeast that delays formation of the prereplicative complex at chromosomal replication origins after exposure to UV light (UVC). This checkpoint absolutely depends on the Gcn2 kinase. Here, we explore the signal for activation of the Gcn2-dependent G_1-S checkpoint in fission yeast. If some form of DNA damage can activate the checkpoint, deficient DNA repair should affect the length of the checkpoint-induced delay. We find that the cell-cycle delay differs in repair-deficient mutants from that in wild-type cells. However, the duration of the delay depends not only on the repair capacity of the cells, but also on the nature of the repair deficiency. First, the delay is abolished in cells that are deficient in the early steps of repair. Second, the delay is prolonged in repair mutants that fail to complete repair after the incision stage. We conclude that the G_1-S delay depends on damage to the DNA and that the activating signal derives not from the initial DNA damage, but from a repair intermediate(s). Surprisingly, we find that activation of Gcn2 does not depend on the processing of DNA damage and that activated Gcn2 alone is not sufficient to delay entry into S phase in UVC-irradiated cells. Thus, the G_1-S delay depends on at least two different inputs.

excision repair | Rad3 | pyrimidine dimers | *Schizosaccharomyces pombe*

Proliferating cells go through a repetitive series of events known as the cell cycle. The progression from one cell-cycle phase to the next is tightly regulated. Cell-cycle progression is monitored and inhibited by checkpoint mechanisms that preserve the correct order of events (1). Some checkpoints are activated by DNA-damaging agents ("DNA damage checkpoints"), and the accompanying cell-cycle delay allows time for damaged DNA to be repaired. Therefore, checkpoints prevent accumulation of mutations and genome instability, which may lead to cancer development (2). Progression through G_1 phase is under particularly tight control because during G_1, the cells can choose between alternative developmental pathways. Entry into S phase is carefully regulated and, in most organisms, under the control of a G_1-S checkpoint. The critical importance of this cell-cycle transition is underlined by the fact that most cancer cells are defective in the G_1-S checkpoint (3–5).

The cell cycle of the model organism *Schizosaccharomyces pombe* is regulated by checkpoints, such as the intra-S, the S-M, and the G_2-M checkpoint that monitor the DNA replication status and the presence of DNA damage (6–8). These checkpoints are largely conserved through evolution. We have described a G_1-S checkpoint in fission yeast that delays formation of the prereplicative complex (preRC) at chromosomal replication origins (9) and absolutely depends on the Gcn2 kinase (10), which is a regulator of translation. The only known mechanism of action of Gcn2 is phosphorylation of the initiation factor eIF2α, which inhibits initiation of translation when phosphorylated.

In all cases previously examined, Gcn2 activation (eIF2α phosphorylation) and delayed entry into S phase correlate, but a causal relationship has not been demonstrated (11). Certain DNA-damaging agents activate the Gcn2-dependent checkpoint, whereas others do not, arguing that it is not a general DNA-damage–inducible checkpoint. However, it does not exclude the possibility that some form(s) of DNA damage can trigger the checkpoint.

It is important to identify the molecular nature of the checkpoint trigger for at least two reasons: First, there is little information about such triggers for any checkpoint. Second, the most obvious possibility is DNA damage and DNA-damage checkpoints are the first barrier against cancer (12, 13). The best-studied checkpoint-activating signal is that for activation of homologs of the ATR kinase. A generally accepted view is that these checkpoint proteins can be activated by single-stranded DNA coated with replication protein A (RPA) (14). Generation of this signal requires damage processing by nucleotide excision repair (NER) (15–17) or by resection of single strands at sites of DNA double-strand breaks (18, 19).

Here, we explore the signal for activation of the Gcn2-dependent G_1-S checkpoint in fission yeast after exposure to UV light (UVC). If DNA damage can activate the checkpoint, we expected DNA-repair–deficient mutants to display a longer checkpoint-induced delay. We show here that the checkpoint delay correlates with the repair capacity of the cells in some repair mutants, strongly suggesting that the checkpoint signal derives from DNA damage. However, the activating signal is not generated in mutants deficient in the earliest stages of DNA repair, arguing that it derives not from the initial damage, but from a repair intermediate(s). Surprisingly, activation of Gcn2 can be uncoupled from the cell-cycle delay in certain DNA-repair mutants, leading us to conclude that although Gcn2 activation is necessary for the cell-cycle delay, it is not sufficient.

Results

Cell-Cycle Delay and DNA Repair in Wild-Type Cells. The dominating damage to DNA after exposure to UVC is formation of cyclobutane pyrimidine dimers (CPDs), and their removal is crucial for cell survival. To explore whether DNA damage and/or its repair is important for checkpoint activation, we measured the repair kinetics of radiation-induced CPDs in wild-type and mutant cells. To this end, we monitored the level of remaining CPDs in the *ade6* locus, using the CPD-specific enzyme T4-endonuclease V (20) (*Materials and Methods* and Fig. S1). All experiments were performed in cells synchronized in G_1 phase by using a *cdc10* arrest, UVC-irradiated, and released into the cell cycle. The initial level of CPDs immediately after irradiation was between 0.2 and 0.3 CPDs per kb in both the transcribed (TS) and nontranscribed (NTS) strand of *ade6*. In repair-proficient wild-type cells, the CPDs were removed with similar kinetics

Author contributions: F.T., E.B., and B.G. designed research; C.A.B., M.K., G.E.R., C.C., O.M., and B.G. performed research; C.A.B., M.K., G.E.R., O.M., F.T., E.B., and B.G. analyzed data; and E.B. and B.G. wrote the paper.

The authors declare no conflict of interest.

*This Direct Submission article had a prearranged editor.

[1]Present address: Neubrunnenstrasse 112, CH-8050 Zürich, Switzerland.

[2]To whom correspondence should be addressed. E-mail: ebo@rr-research.no.

This article contains supporting information online at www.pnas.org/lookup/suppl/doi:10.1073/pnas.1204901109/-/DCSupplemental.

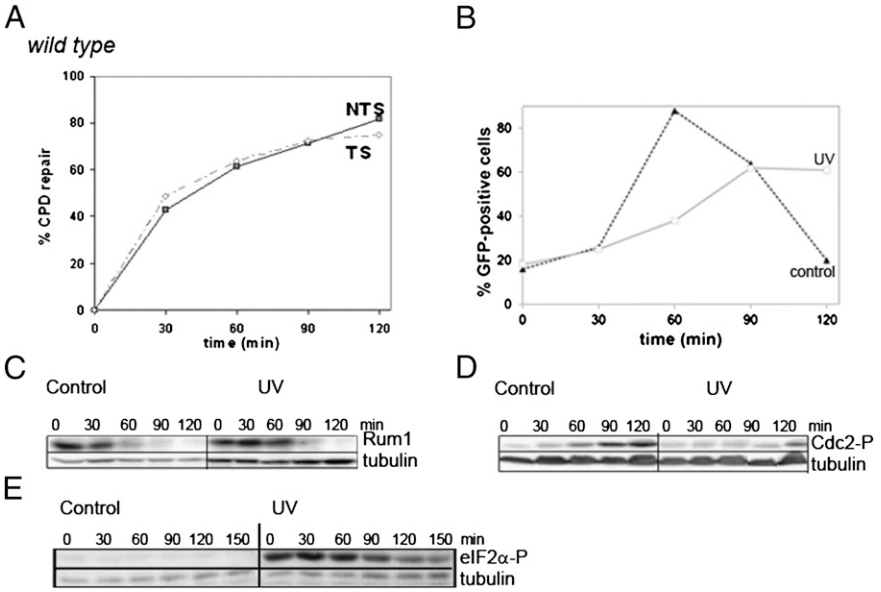

Fig. 1. CPD repair and cell-cycle progression in wild-type cells. (*A*) Quantitative analysis of the CPD repair in the *ade6* locus (XhoI fragment) from Southern blots (Fig. S1*A*) of genomic DNA isolated at different times after UVC irradiation: transcribed (TS) and nontranscribed (NTS) strand. (*B*) Percentage of cells that contained chromatin-bound Mcm7-GFP (preRC) at different timepoints after release into the cell cycle. Data for unirradiated control cells are plotted by using filled symbols and dashed lines; data for UV-irradiated cells are plotted using open symbols and solid lines. (*C–E*) Immunoblots of total cell extracts from UVC-irradiated wild-type cells, probed with antibody against Rum1 (*C*), phosphorylated Cdc2 (*D*), and phosphorylated eIF2α (*E*). The presence of tubulin was used as loading control.

from both strands (Fig. 1*A*). Approximately 60% of the dimers were removed during 60 min of incubation at 25 °C and approximately 80% was removed in 120 min, consistent with the efficient repair observed earlier (21).

We have shown that cells UVC-irradiated in G_1 phase delay entry into S phase because of the Gcn2-dependent G_1-S checkpoint and, subsequently, delay DNA replication, presumably when the replication forks reach DNA lesions. Three assays were used to discriminate between cells in G_1 and S phase in the present work: the loading of the preRC onto chromatin and the presence of Rum1 and phosphorylated Cdc2 (22). The preRC formation is essential for the initiation of DNA replication and occurs in G_1 phase. The frequency of cells displaying preRC formation, as measured by the presence of chromatin-bound GFP-tagged Mcm7 (23), was maximal 60 min after the release of unirradiated control cells and at 90–100 min in cells exposed to UVC (Fig. 1*B* and ref. 10). Note that cells arrested in S phase contain chromatin-bound Mcms, giving rise to a plateau rather than a peak of preRC-positive cells after UVC irradiation. Rum1 is an inhibitor of Cdc2 and is only present in G_1 phase (24–26), whereas Cdc2 is present throughout the cell cycle, but becomes phosphorylated at Tyr15 as the cells enter S phase (27, 28). In nonirradiated control cells, Rum1 was degraded already at 60 min (Fig. 1*C*), in agreement with previous data (10). This event occurred at about the same time as Cdc2 became phosphorylated (Fig. 1*D*), consistent with the preRC data and with the conclusion that this is the time when unirradiated cells enter S phase (9). In cells exposed to UVC, Rum1 disappeared later, 90 min after irradiation, and Cdc2 phosphorylation was detectable only after 120 min (Fig. 1 *C* and *D*). These data show, as seen before (10), that the cells delay S-phase entry for more than 30 min in response to UVC irradiation and that the three parameters give consistent reports on cell-cycle progression. The phosphorylation of eIF2α was monitored as a measure of Gcn2 activation and it coincided with the length of the cell-cycle delay (Fig. 1*E*). We have shown that UVC-induced eIF2α phosphorylation and the cell-cycle delay are abolished in the absence of Gcn2 (10).

Excision Repair in Fission Yeast. Fission yeast contains a classic NER pathway and, in addition, the UV-damaged DNA endonuclease-dependent excision repair (UVER) pathway (29). Like for most organisms, NER consists of two subpathways: the transcription-coupled repair (TCR), which removes damage from the transcribed strand of actively transcribed genes and the global genome repair (GGR), which removes damage from the genome overall. In most cell types, repair through the TCR pathway occurs more rapidly than through the GGR pathway (21, 30). In *S. pombe* the UVER pathway apparently repairs CPDs equally well on transcribed and nontranscribed strands and, importantly, at a much higher rate than NER does (21, 29, 30).

Both NER and UVER start by recognition of the lesion, followed by endonuclease incision next to the lesion, excision, resynthesis and ligation (Fig. 2). In analogy to NER in human and budding yeast cells the XPA/Rad14 homolog Rhp14 has

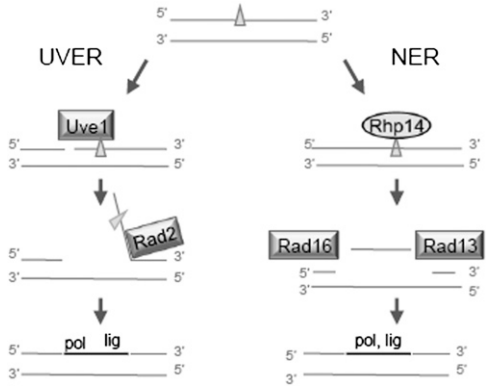

Fig. 2. Removal of UVC-induced DNA damage in fission yeast. The major steps of NER and UVER are shown, and the points of action of the genes used in this work are indicated.

a role in damage recognition, whereafter the endonucleases Rad16 and Rad13 make cuts on either side of the lesion (31–33). Then the oligonucleotide containing the lesion is removed by a helicase, followed by resynthesis and ligation. The UVER pathway (Fig. 2) is initiated by the Uve1 endonuclease (34, 35), whereafter a flap-structure containing the lesion is created by helicase activity and the flap is released by the endonuclease Rad2 (21). Finally, resynthesis and ligation complete the repair pathway.

No G_1 Delay in the *rhp14 uve1* Mutant. To test whether DNA damage is important for checkpoint activation, we measured CPD repair and cell-cycle delay in mutants with different capacities for DNA repair. Deletion of the genes encoding the initiating proteins Rhp14 (NER) and Uve1 (UVER) was expected to prevent excision repair altogether. As expected, no CPD removal was detected in the *rhp14 uve1* mutant (Fig. S2). Remarkably, the UVC-induced G_1 delay is strongly reduced and almost abolished, because preRC loading occurs with very little delay after irradiation (see Figs. 3*A* and 6). Consistently, Rum1 levels are markedly reduced at the same early point in time and Cdc2 phosphorylation also occurs early and regardless of UVC exposure (Fig. 3 *B* and *C*). We conclude that these cells enter S phase without activating a G_1-S checkpoint. These results suggest that the cell-cycle delay depends on DNA damage and not on damage to other macromolecules. Furthermore, checkpoint activation requires either recognition of the DNA damage or a biochemical step downstream of recognition. Surprisingly, the remarkable effect on cell-cycle progression by removing both Rhp14 and Uve1 is not accompanied by a reduced duration of eIF2α phosphorylation (Fig. 3*D*). In the mutant lacking both repair proteins, eIF2α remains phosphorylated after the cells have entered S phase, and there seems to be no correlation among checkpoint induction, S-phase entry, and eIF2α phosphorylation.

Strongly Reduced G_1 Delay in the *rad16 rad13 uve1* Mutant. To address whether DNA damage recognition is sufficient to activate the checkpoint, we used a *rad16 rad13 uve1* mutant where all incision activity is abolished, but where damage recognition by Rhp14 is retained. Like for the *rhp14 uve1* mutant cells (above), preRC loading occurred with only a short delay, if any, after UVC exposure (see Figs. 4*A* and 6), indicating that checkpoint activation is impaired. Consistently, Rum1 is degraded and Cdc2 is phosphorylated with about the same timing in irradiated and unirradiated cells (Fig. 4 *B* and *C*). These data strongly argue that full checkpoint activation requires damage processing at least up to the incision step and most likely beyond. In the *rad16 rad13 uve1* cells, eIF2α is phosphorylated (Fig. 4*D*) with the same timing as in repair-proficient (Fig. 1*E*) and *rhp14 uve1* cells (Fig. 3*D*). Therefore, in these mutant cells, Gcn2 activation occurs in the absence of DNA-damage processing and is uncoupled from the cell-cycle delay.

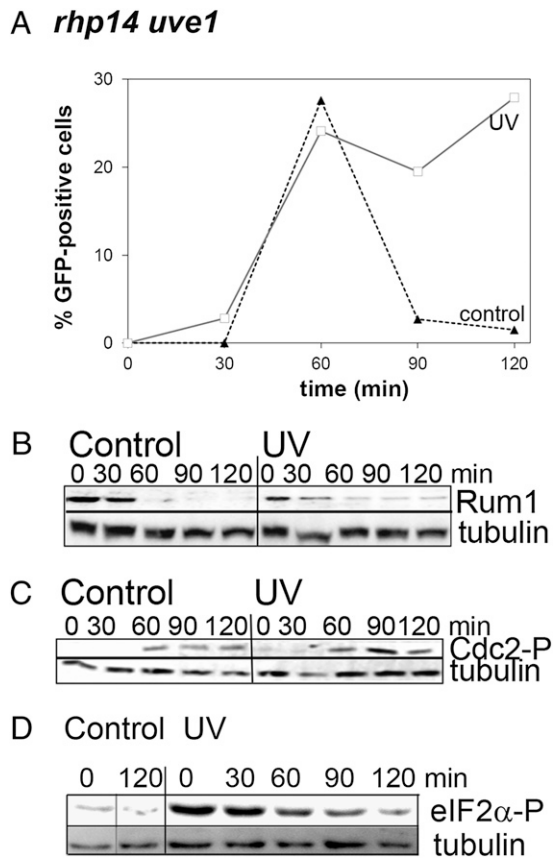

Fig. 3. Cell-cycle progression in the *rhp14 uve1* mutant. (*A*) Percentage of cells that contained chromatin-bound pre-RC at different timepoints after release into the cell cycle. Symbols are as in Fig. 1*B*. (*B–D*) Immunoblots of total cell extracts from UVC-irradiated *rhp14 uve1* cells, probed with antibody against Rum1 (*B*), phosphorylated Cdc2 (*C*), and phosphorylated eIF2α (*D*). The presence of tubulin was used as loading control. The gray line in *D* indicates that intervening timepoints have been removed.

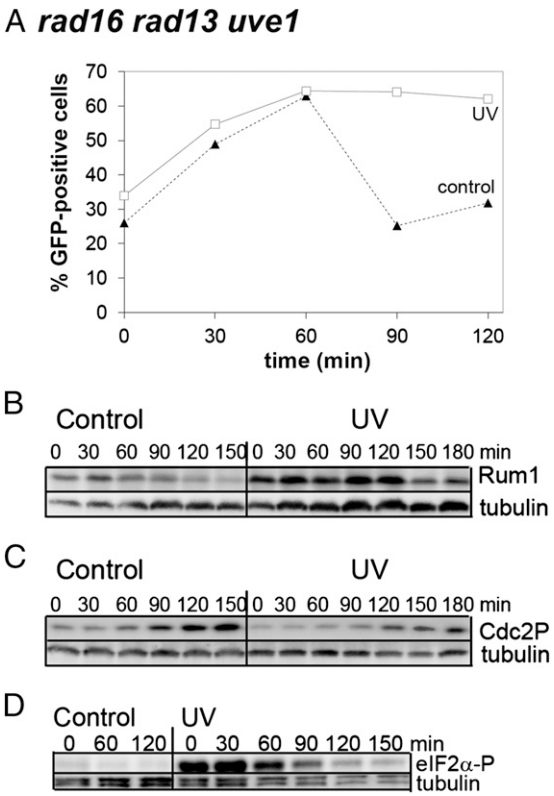

Fig. 4. Cell-cycle progression in the *rad16 rad13 uve1* mutant. (*A*) Percentage of cells that contained chromatin-bound pre-RC at different timepoints after release into the cell cycle. Data for unirradiated control cells are plotted by using filled symbols and dashed lines; data for UV-irradiated cells are plotted using open symbols and solid lines. (*B–D*) Immunoblots of total cell extracts from UVC-irradiated *rad16 rad13 uve1* cells, probed with antibody against Rum1 (*B*), phosphorylated Cdc2 (*C*), and phosphorylated eIF2α (*D*). The presence of tubulin was used as loading control.

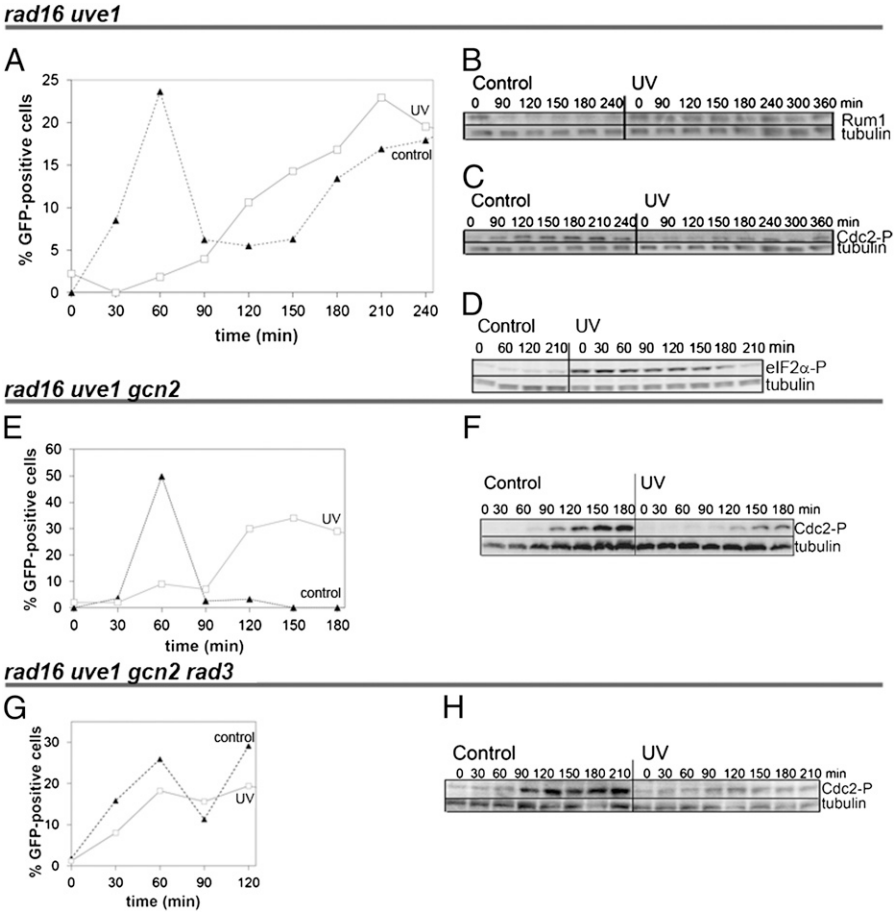

Fig. 5. CPD repair and cell-cycle progression in the *rad16 uve1* mutant. (*A*) Percentage of *rad16 uve1* cells that contained chromatin-bound pre-RC at different timepoints after release into the cell cycle. Data for unirradiated control cells are plotted by using filled symbols and dashed lines for all graphs; data for UV-irradiated cells are plotted using open symbols and solid lines. (*B–D*) Immunoblots of total cell extracts from UVC-irradiated *rad16 uve1* cells, probed with antibody against Rum1 (*B*), phosphorylated Cdc2 (*C*), and phosphorylated eIF2α (*D*). The presence of tubulin was used as loading control. (*E*) Percentage of *rad16 uve1 gcn2* cells that contained chromatin-bound Mcm7-GFP (pre-RC) at different timepoints after release into the cell cycle. (*F*) Immunoblots of total cell extracts from UVC-irradiated *rad16 uve1 gcn2* cells, probed with antibody against phosphorylated Cdc2. The presence of tubulin was used as loading control. (*G*) Percentage of *rad16 uve gcn2 rad3* cells that contained chromatin-bound pre-RC at different timepoints after release into the cell cycle. (*H*) Immunoblots of total cell extracts from UVC-irradiated *rad16 uve1 gcn2 rad3* cells, probed with antibody against phosphorylated Cdc2. The presence of tubulin was used as loading control.

Prolonged G_1 Delay in the *rad16 uve1* and *rad13 uve1* Mutants. An equally repair-deficient double mutant as those above is *rad16 uve1*, in which no CPD removal could be detected for at least 4 h after UVC (Fig. S3). The irradiated mutant cells arrested in G_1 for over 3 h, as seen by the delayed loading of the preRC (Figs. 5*A* and 6), by the continued presence of Rum1 and by the delayed Cdc2 phosphorylation (Fig. 5 *B* and *C*). Similarly, in the *rad13 uve1* mutant, very little CPD removal could be detected (Fig. S4*A*). The *rad13 uve1* cells entered S phase with a delay of 60–80 min as shown by a delayed preRC loading (Fig. S4*B* and Fig. 6) and a delayed Cdc2 phosphorylation (Fig. S4*C*). The long UVC-induced G_1 delay in the *rad16 uve1* and in the *rad13 uve1* mutants compared with no delay in *rad16 rad13 uve1* indicates that the delay depends on processing the damage at least up to and including the incision step.

Importantly, phosphorylation of eIF2α was maintained about as long as in wild-type cells in both these mutants (Fig. 5*D* and Fig. S4*D*) and, therefore, did not correlate with the length of the cell-cycle delay.

Deletion of *gcn2* Reduces but Does Not Abolish the Prolonged G_1 Delay. To explore the role of Gcn2 in the prolonged delay of the *rad16 uve1* mutant, we measured the length of the G_1 delay in the *rad16 uve1 gcn2* mutant after exposure to UVC. PreRC loading in irradiated cells occurred 60 min later than in unirradiated cells (Figs. 5*E* and 6), consistent with the appearance of phosphorylated

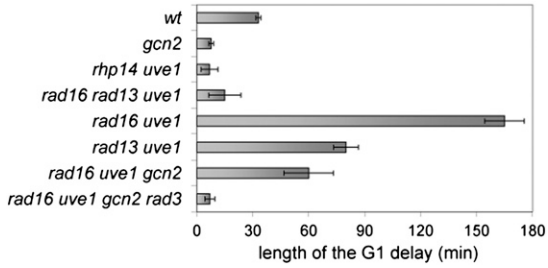

Fig. 6. Cell-cycle progression after UVC irradiation in the investigated mutants. The percentage of cells containing chromatin-bound Mcm was determined as described in *Materials and Methods* in at least three independent experiments. The delay was determined as the time difference at reaching maximal preRC loading between irradiated and unirradiated cells. We have published that *gcn2* cells have no UVC-induced delay (10), and a summary of these previously published data are shown here for comparison.

Cdc2 at 150 min after irradiation versus at 90 min in control cells (Fig. 5*F*). This delay is significantly shorter than that found in the otherwise isogenic *gcn2*$^+$ cells (Figs. 5 *A–C* and 6). We conclude that the prolonged cell-cycle delay of the *rad16 uve1* mutant is reduced, but not completely abolished, in the absence of Gcn2. Therefore, a part of the prolonged delay is Gcn2-dependent.

The G_1 Delay Is Abolished in the *rad16 uve1 gcn2 rad3* Mutant. The presence of a Gcn2-independent G_1 delay in the *rad16 uve1* mutant suggests the existence of an additional mechanism that delays entry into S phase. To address the involvement of the classic checkpoint protein Rad3, we monitored S-phase entry after UVC irradiation of the *rad16 uve1 gcn2 rad3* mutant cells. PreRC loading occurred with the same kinetics in control and irradiated cells (Fig. 5*G*), suggesting that the remaining delay observed in *rad16 uve1 gcn2* is due to the activation of a Rad3-dependent pathway. Consistently, Cdc2 phosphorylation occurred at the same time in control and irradiated cells, at 90 min (Fig. 5*H*). In the irradiated cells, Cdc2 soon becomes dephosphorylated again, most likely because in the absence of Rad3 and the S-M checkpoint, the irradiated cells enter mitosis prematurely.

Discussion

Most organisms display checkpoints that arrest the cell-cycle progression after exposure to DNA-damaging agents, but the molecular signal(s) inducing the checkpoints are in most instances not known. Here, we have investigated the inducing signal for the G_1-S checkpoint in fission yeast.

G_1-S Delay Requires Processing of UVC-Induced Lesions. The *rhp14 uve1* double mutant displayed a strongly reduced UVC-inducible G_1 delay compared with that observed in wild-type cells (Fig. 6). The most likely explanation is that in the absence of Rhp14 and Uve1, the UVC-induced DNA damage is not recognized, which, in turn, leads to a lack of checkpoint induction. Thus, our data implicate a link between ongoing DNA repair and checkpoint induction. An alternative explanation for *rhp14 uve1* losing the checkpoint is that the Rhp14 and/or Uve1 proteins themselves signal to activate the checkpoint. This explanation is unlikely because the checkpoint is also defective in the *rad16 rad13 uve1* mutant (Fig. 6) where Rhp14 is present. Our data strongly argue that one or more of the repair intermediates induce the checkpoint.

The presence of one endonuclease (either Rad13 or Rad16) resulted in checkpoint activation, strongly suggesting that incision is a critical step to generate the activating signal. Furthermore, because either endonuclease is able to activate the checkpoint, it appears that either of them can cleave independently of the other. This finding is in contrast to observations in human cells, where the 3′ incision depends on a prior 5′ incision (36). Interestingly, the presence of either the 5′ or 3′ NER-endonuclease resulted in cell-cycle delays of slightly different durations, suggesting that the length of the delay is determined by how the incision is processed. In the *rad16 uve1* mutant, Rad13 seems to be able to make an incision 3′ to the lesion. The damaged strand might be displaced by a helicase to generate single-stranded DNA required for activation of Rad3. However, the single-strand gap cannot be readily filled by DNA repair synthesis, because there is no 3′ OH group that can be extended. In the *rad13 uve1* mutant, Rad16 appears to make an incision 5′ to the lesion, which might initiate repair synthesis in the absence of the 3′ incision, as was shown for human cells (36). It is likely that this difference in processing of lesions is the reason for the longer delay in the *rad16 uve1* mutant than in the *rad13 uve1* cells.

Activation of Gcn2 Is Necessary but Not Sufficient for the G_1-S Checkpoint. Here we have shown that Gcn2 activation, measured as eIF2α phosphorylation, does not always correlate with the observed cell-cycle delay. First, in two repair-deficient mutants (*rhp14 uve1* and *rad16 rad13 uve1*) the duration of eIF2α phosphorylation after UVC was as long as for wild-type cells, but the cell-cycle delay was considerably shorter or absent (Fig. 6). Second, in the repair-deficient *rad16 uve1* and *rad13 uve1* mutants the period of eIF2α phosphorylation was similar to that found in wild-type cells, whereas the duration of the cell-cycle delay was much longer (Fig. 6). This difference suggests that the signal for Gcn2 activation does not depend on DNA damage or its processing and indicates a different route of activation (Fig. 7). Furthermore, activation of Gcn2 is not sufficient to produce a G_1 delay, although Gcn2 is absolutely required for the checkpoint both in wild-type cells (10) and in repair-deficient cells (Fig. 6). We conclude that the length of the G_1 delay depends on at least two different inputs: activation of Gcn2 and processing of DNA damage. We suggest that Gcn2 is essential for the DNA-damage-dependent pathway (Fig. 7), possibly by maintaining efficient translation of some of the components.

Incomplete Repair of DNA Damage Can Induce a Rad3-Dependent G_1 Delay. Surprisingly, the long delay in *rad16 uve1* cells was not completely abolished in the absence of Gcn2 (Fig. 6). The remaining delay is due to the activity of Rad3, because there was no delay in the *rad3 gcn2 rad16 uve1* mutant (Fig. 6). G_1-S checkpoints have been described in most organisms, but little is known about their initiating signals and the targets. UVC irradiation of *Saccharomyces cerevisiae* cells induces a checkpoint that arrests the cells in G_1 and activates the ATR and Rad3 homolog Mec1 (37). Similarly, in human cells, an ATR-dependent checkpoint is activated by UVC in G_1 (38). No Rad3-dependent G_1-S checkpoint has been described in fission yeast. Here, we show that Rad3 can contribute to a G_1 delay in a repair-deficient mutant and it remains to be seen whether it can also do so in wild-type cells.

We have shown that fission yeast cells delay entry into S phase after UVC irradiation by a Gcn2-dependent mechanism (10). Here, we demonstrate that this radiation-induced delay in G_1 phase depends on processing of the DNA damage. The DNA repair must proceed at least past the incision step. This observation is similar to the findings that in *S. cerevisiae* and human cells the Mec1/ATR-dependent checkpoints require NER activity (15–17). Thus, a common strategy for generating the activating signal for the G_1-S checkpoints appears to involve damage processing by the prevalent repair mechanisms. Furthermore, activation of Gcn2 does not depend on processing DNA damage and the inducing signal remains to be identified. We conclude that the G_1-S delay depends on at least two different inputs.

Materials and Methods

Yeast Strains and Cell Handling. All of the strains are derivatives of the *S. pombe* L972 h$^-$ strain. The strains used are listed in Table S1. Media and growth conditions were as described (39). The cells were grown in liquid

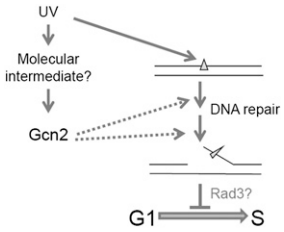

Fig. 7. Induction of a G_1-S checkpoint in fission yeast. A model consistent with all our results. In the absence of Gcn2, the DNA-damage pathway cannot induce the delay. In DNA-repair mutants, the relevant repair intermediate cannot be generated regardless of the presence of Gcn2.

Edinburgh minimal medium (EMM) or yeast extract medium (YE), at 25 °C, to a cell concentration of 2–4 × 10^6/mL (OD_{595} of 0.1–0.2). The cells were synchronized in G_1 phase by incubating *cdc10-M17* cells at 36 °C for 4 h (EMM) or 3 h (YE) before release into the cell cycle at 25 °C.

UVC Irradiation. A dose of 1,100 J/m^2 of UVC irradiation (254 nm) was given at an incident dose rate of approximately 250 J/m^2 per min in a thin, stirred suspension in EMM medium, as described (9). G_1-synchronized cells were irradiated immediately after the release from the *cdc10* block. Samples for analysis of proteins or DNA were collected immediately after irradiation (time 0) and after further incubation at 25 °C.

Immunoblots. Immunoblotting was performed as described (11). The antibodies used were as follows: anti-phospho-Cdc2 (Tyr15; Cell Signaling, 911S) at dilution 1:400; anti-Rum1, 1:500 (a kind gift form S. Moreno); anti-phosphorylated eIF2α (Biosource, no. 44–7282) 1:2,000; and anti-α-tubulin (T-5168 Sigma), 1:30 000.

PreRC Loading. Extraction of unbound MCM proteins was performed as described (23). All experiments were performed at least three times. Representative results are shown in Figs. 1–6; the average of at least three experiments is shown in Fig. 6.

CPD Analysis. Genomic DNA was isolated from UVC-irradiated cells, as described (39). CPD analysis of the XhoI fragment containing the *ade6* gene was done as described (20). Briefly, the genomic DNA was cut to completion with XhoI, cut at CPDs with T4-endonuclease V or mock treated, separated on alkaline agarose gels, blotted, and hybridized to strand-specific probes close to the XhoI site in the *ade6* gene. The probes were made by primer extension using the EcoRI-XhoI DNA of *ade6* as a template and primers 1069 (5′-GTACGGATGTTTTTCAGCTCACCGCACAC-3′) and 1068 (3′GCCTCAACTGAGAGAAGTGAGCTTAAGCCTG-5′) to generate probes that hybridize to the bottom and top strand, respectively. The bottom strand of *ade6* corresponds to the transcribed strand (TS), the top strand to the nontranscribed strand (NTS). Afterward, the blots were stripped and rehybridized with probes detecting the other strand and, in both cases, quantified by using PhosphoImager. The average number of CPDs/restriction fragments were calculated by using the Poisson expression (40).

ACKNOWLEDGMENTS. We thank S. Moreno for the Rum1 antiserum, A. Bucceri and A. Meier for help with the CPD mapping, and L. Lindbergsengen for excellent technical assistance. This work was supported by The Research Council of Norway, the Norwegian Cancer Society, South-Eastern Norway Regional Health Authority, Radiumhospitalets Legater, Eidgenössische Technische Hochschule-Zürich and Swiss National Science Foundation Grants 3100AO-102152 and 3100AO-122033.

1. Hartwell LH, Weinert TA (1989) Checkpoints: Controls that ensure the order of cell cycle events. *Science* 246:629–634.
2. Niida H, Nakanishi M (2006) DNA damage checkpoints in mammals. *Mutagenesis* 21: 3–9.
3. Bartek J, Lukas C, Lukas J (2004) Checking on DNA damage in S phase. *Nat Rev Mol Cell Biol* 5:792–804.
4. Nojima H (2004) G1 and S-phase checkpoints, chromosome instability, and cancer. *Methods Mol Biol* 280:3–49.
5. Sherr CJ, McCormick F (2002) The RB and p53 pathways in cancer. *Cancer Cell* 2: 103–112.
6. Carr AM (2002) DNA structure dependent checkpoints as regulators of DNA repair. *DNA Repair (Amst)* 1:983–994.
7. Cuddihy AR, O'Connell MJ (2003) Cell-cycle responses to DNA damage in G2. *Int Rev Cytol* 222:99–140.
8. Huberman JA (1999) DNA damage and replication checkpoints in the fission yeast, Schizosaccharomyces pombe. *Prog Nucleic Acid Res Mol Biol* 62:369–395.
9. Nilssen EA, Synnes M, Kleckner N, Grallert B, Boye E (2003) Intra-G1 arrest in response to UV irradiation in fission yeast. *Proc Natl Acad Sci USA* 100:10758–10763.
10. Tvegård T, et al. (2007) A novel checkpoint mechanism regulating the G1/S transition. *Genes Dev* 21:649–654.
11. Krohn M, Skjølberg HC, Soltani H, Grallert B, Boye E (2008) The G1-S checkpoint in fission yeast is not a general DNA damage checkpoint. *J Cell Sci* 121:4047–4054.
12. Bartkova J, et al. (2005) DNA damage response as a candidate anti-cancer barrier in early human tumorigenesis. *Nature* 434:864–870.
13. Bartek J, Bartkova J, Lukas J (2007) DNA damage signalling guards against activated oncogenes and tumour progression. *Oncogene* 26:7773–7779.
14. Zou L, Elledge SJ (2003) Sensing DNA damage through ATRIP recognition of RPA-ssDNA complexes. *Science* 300:1542–1548.
15. Bomgarden RD, et al. (2006) Opposing effects of the UV lesion repair protein XPA and UV bypass polymerase eta on ATR checkpoint signaling. *EMBO J* 25:2605–2614.
16. Giannattasio M, Lazzaro F, Longhese MP, Plevani P, Muzi-Falconi M (2004) Physical and functional interactions between nucleotide excision repair and DNA damage checkpoint. *EMBO J* 23:429–438.
17. Marini F, et al. (2006) DNA nucleotide excision repair-dependent signaling to checkpoint activation. *Proc Natl Acad Sci USA* 103:17325–17330.
18. Dubrana K, van Attikum H, Hediger F, Gasser SM (2007) The processing of double-strand breaks and binding of single-strand-binding proteins RPA and Rad51 modulate the formation of ATR-kinase foci in yeast. *J Cell Sci* 120:4209–4220.
19. Shiotani B, Zou L (2009) Single-stranded DNA orchestrates an ATM-to-ATR switch at DNA breaks. *Mol Cell* 33:547–558.
20. Suter B, Livingstone-Zatchej M, Thoma F (1999) Mapping cyclobutane-pyrimidine dimers in DNA and using DNA-repair by photolyase for chromatin analysis in yeast. *Methods Enzymol* 304:447–461.
21. Yasuhira S, Morimyo M, Yasui A (1999) Transcription dependence and the roles of two excision repair pathways for UV damage in fission yeast Schizosaccharomyces pombe. *J Biol Chem* 274:26822–26827.
22. Boye E, Skjølberg HC, Grallert B (2009) Checkpoint regulation of DNA replication. *Methods Mol Biol* 521:55–70.
23. Kearsey SE, Montgomery S, Labib K, Lindner K (2000) Chromatin binding of the fission yeast replication factor mcm4 occurs during anaphase and requires ORC and cdc18. *EMBO J* 19:1681–1690.
24. Benito J, Martín-Castellanos C, Moreno S (1998) Regulation of the G1 phase of the cell cycle by periodic stabilization and degradation of the p25rum1 CDK inhibitor. *EMBO J* 17:482–497.
25. Correa-Bordes J, Gulli MP, Nurse P (1997) p25rum1 promotes proteolysis of the mitotic B-cyclin p56cdc13 during G1 of the fission yeast cell cycle. *EMBO J* 16:4657–4664.
26. Moreno S, Labib K, Correa J, Nurse P (1994) Regulation of the cell cycle timing of Start in fission yeast by the rum1+ gene. *J Cell Sci Suppl* 18:63–68.
27. Hayles J, Nurse P (1995) A pre-start checkpoint preventing mitosis in fission yeast acts independently of p34cdc2 tyrosine phosphorylation. *EMBO J* 14:2760–2771.
28. Zarzov P, Decottignies A, Baldacci G, Nurse P (2002) G(1)/S CDK is inhibited to restrain mitotic onset when DNA replication is blocked in fission yeast. *EMBO J* 21:3370–3376.
29. Yonemasu R, et al. (1997) Characterization of the alternative excision repair pathway of UV-damaged DNA in Schizosaccharomyces pombe. *Nucleic Acids Res* 25:1553–1558.
30. Lombaerts M, Tijsterman M, Brandsma JA, Verhage RA, Brouwer J (1999) Removal of cyclobutane pyrimidine dimers by the UV damage repair and nucleotide excision repair pathways of Schizosaccharomyces pombe at nucleotide resolution. *Nucleic Acids Res* 27:2868–2874.
31. Carr AM, et al. (1994) The rad16 gene of Schizosaccharomyces pombe: A homolog of the RAD1 gene of Saccharomyces cerevisiae. *Mol Cell Biol* 14:2029–2040.
32. McCready S, Carr AM, Lehmann AR (1993) Repair of cyclobutane pyrimidine dimers and 6-4 photoproducts in the fission yeast Schizosaccharomyces pombe. *Mol Microbiol* 10:885–890.
33. McCready SJ, Yasui A, Yasui A (2000) Repair of UV damage in the fission yeast Schizosaccharomyces pombe. *Mutat Res* 451:197–210.
34. Kanno S, Iwai S, Takao M, Yasui A (1999) Repair of apurinic/apyrimidinic sites by UV damage endonuclease; a repair protein for UV and oxidative damage. *Nucleic Acids Res* 27:3096–3103.
35. Avery AM, et al. (1999) Substrate specificity of ultraviolet DNA endonuclease (UVDE/Uve1p) from Schizosaccharomyces pombe. *Nucleic Acids Res* 27:2256–2264.
36. Staresincic L, et al. (2009) Coordination of dual incision and repair synthesis in human nucleotide excision repair. *EMBO J* 28:1111–1120.
37. Siede W, Friedberg AS, Dianova I, Friedberg EC (1994) Characterization of G1 checkpoint control in the yeast Saccharomyces cerevisiae following exposure to DNA-damaging agents. *Genetics* 138:271–281.
38. Tibbetts RS, et al. (1999) A role for ATR in the DNA damage-induced phosphorylation of p53. *Genes Dev* 13:152–157.
39. Moreno S, Klar A, Nurse P (1991) Molecular genetic analysis of fission yeast Schizosaccharomyces pombe. *Methods Enzymol* 194:795–823.
40. Mellon I, Spivak G, Hanawalt PC (1987) Selective removal of transcription-blocking DNA damage from the transcribed strand of the mammalian DHFR gene. *Cell* 51: 241–249.